PREDICTION OF THERMOACOUSTIC INSTABILITIES IN COMBUSTORS USING LINEARIZED NAVIER-STOKES EQUATIONS IN FREQUENCY DOMAIN

Wei Na, Gunilla Efraimsson and Susann Boij
Department of Aeronautical and Vehicle Engineering
Royal Institute of Technology, Stockholm, Sweden
Linné FLOW Centre, Stockholm, Sweden
ECO2 Vehicle Design Centre, Stockholm, Sweden
Email: wein@kth.se

The paper presents a numerical methodology for the prediction of thermoacoustic instabilities with the effects of mean flow as well as the viscous effect. As an academic benchmark, the Rijke tube configuration with the flame sheet located in the middle of the duct is used for validating the numerical methodology. The numerical methodology of solving linearized Navier-Stokes equations (LNSE) in frequency domain with the steady heat release is described in the paper. The numerical results are compared to the semi-analytical results by Dowling [1].

1. Introduction

Combustion instabilities usually refer to the sustained high-amplitude pressure oscillations which can lead to the structural damage of the combustors in aero-engines. These self-excited oscillations are due to the coupling between the fluctuation of the heat release rate and the pressure perturbations. More specifically, there is a feedback process in the combustors which can relate the downstream flow to the upstream region where the perturbations are generated. Usually the acoustic propagation is responsible for the feedback process, while the coupling may also involve convective modes such as entropy mode and vorticity mode. For instance, when the entropy wave is propagating upon a nozzle end of a pipe, it will generate the acoustic wave [2] which may result in the change of the flame front position or the instantaneous heat release rate. Vorticity wave plays an significant role in the acoustic boundary layer which could lead to the flashback of the flame [3]. Also, some energy will be transferred from the acoustic mode to vorticity mode. It is important to understand the interaction between combustion and waves or flow perturbations, which may become driving or coupling processes under the unstable conditions.

The advantage of using linearized Navier-Stokes equation (LNSE) to predict thermoacousic instabilities is to take into account the acoustic mode as well as the entropy mode and the vorticity mode. Compared to the existing numerical methods, Large eddy simulation (LES), Direct numerical simulation (DNS) or low order methods, LNSE is much less computational demanding and can be applied to extensive numerical geometries [4], even three-dimensional ones. Some numerical work has been carried out by solving linearized euqations, e.g., F. Nicoud has investigated the influence of the mean flow on the thermoacoustic instabilities by solving linearied Euler equations (LEE) [5]. D. Iurashev has predicted the limit cycle of the instabilities by solving the LNSE in the time domain [6]. J. Gikadi has predicted the acoustic modes in combustors by solving the LNSE in the frequency domain [7]. Compared with Gikadi's work, this paper reformulates a different form of energy equation and the entropy perturbations can be directly obtained rather than solving the pressure perturbations.

For the prediction of thermoacoustic instabilities, the wave propagation over a baseline flow gives rise to an eigenvalue problem [5]. The complex eigenvalues are related to the frequencies of the thermoacoustic modes and the growth rate. The mathematical formulations presented in this paper are solved as an eigenvalue problem with the discretazation of Finite Element Method (FEM).

2. Mathematical model

In this section, the mathematical formulations of LNSE in frequency domain are presented including the basic equations, the linearizations, the harmonic equations, and the eigenvalue matrix.

2.1 Basic Navier-Stokes equations with assumptions

The basic governing equations are the Navier-Stokes equations, which includes the continuity equation, the momentum equations as well as the energy equation. One should consider the following assumptions: an homogeneous reacting mixture with constant heat capacities C_p and C_v; the mixture is a perfect gas; body forces are neglected and the flow is adiabatic [5].

The continuity and the momentum equations are present respectively as below:

$$\frac{\mathrm{D}\rho}{\mathrm{D}t} = -\rho\frac{\partial u_i}{\partial x_i} \tag{1}$$

$$\rho\frac{\mathrm{D}u_i}{\mathrm{D}t} = -\frac{\partial p}{\partial x_i} + \frac{\partial \tau_{ij}}{\partial x_j} \tag{2}$$

By neglecting the body forces and the heat conduction, the energy equation in terms of total energy is presented as Eq. (3) [8].

$$\rho\frac{\mathrm{D}}{\mathrm{D}t}\left(e + \frac{u_i u_i}{2}\right) = \rho\dot{q} - \frac{\partial(pu_i)}{\partial x_i} + \frac{\partial(u_i\tau_{ij})}{\partial x_j} \tag{3}$$

However, the energy equation could be reformulated in several different forms depending on which variables are primarily concerned to be solved. For example, when a flame is present, the entropy field couples with the acoustic perturbations to generate hot spots. In this case, entropy waves can play an significant role for combustion instabilities [9]. It is also very important to develop a numerical methodology in consideration of the physical phenomenon in combustors. For these reasons, the energy equation in terms of entropy is given as Eq. (4):

$$\frac{\mathrm{D}s}{\mathrm{D}t} = \frac{R}{p}(\dot{q} + \tau_{ij}\frac{\partial u_i}{\partial x_j}) \tag{4}$$

In some situations, for the convenience of comparing numerical results with the experimental results, the energy equation can also be formulated in terms of the pressure as Eq. (5):

$$\frac{\partial p}{\partial t} + u_i\frac{\partial p}{\partial x_i} + \gamma p\frac{\partial u_i}{\partial x_i} = (\gamma - 1)\left(\dot{q} + \tau_{ij}\frac{\partial u_i}{\partial x_j}\right) \tag{5}$$

In Eq. (1) to Eq. (5), ρ, u_i, p and s stand for the mixture density, i component of the velocity in the Cartesian coordinates, static pressure and entropy per mass unit respectively. In addition, e is the internal energy per unit mass, $\dot{q}$ is the rate of heat release per unit of volume, $R = 287J/(kg \cdot K)$ is the constant specific gas constant, γ is the heat capacity ratio and τ_{ij} is the viscous stress and defined as:

$$\tau_{ij} = \mu\left(\frac{\partial u_i}{\partial x_j} + \frac{\partial u_j}{\partial x_i} - \frac{2}{3}\frac{\partial u_k}{\partial x_k}\delta_{ij}\right) \tag{6}$$

where δ_{ij} is the Kronecker delta function and μ is the dynamic viscosity.

For the ideal gas mixture, the state equation and the entropy expression are given as:

$$p = \rho RT \tag{7}$$

$$s - s_{ref} = C_v ln\left(\frac{p}{p_{ref}}\right) - C_p ln\left(\frac{\rho}{\rho_{ref}}\right) \tag{8}$$

where, T is the temperature, C_v is the specific heat at constant volume, C_p is the specific heat at constant pressure and the subscript 'ref' index stands for standard values.

2.2 Linearization of the Navier-Stokes equations

Assuming each variable can be written as a composition of a mean flow and a small perturbation, such as: $\rho = \bar{\rho} + \rho'$, $u_i = \bar{u}_i + u'_i$, $p = \bar{p} + p'$, $s = \bar{s} + s'$, $\tau_{ij} = \bar{\tau}_{ij} + \tau'_{ij}$, $\dot{q} = \bar{\dot{q}} + \dot{q}'$. Introducing the preceding expansions into the Eq. (1) - Eq. (4) and keeping only terms of the first order, the linearized equations for perturbations taking into account the steady heat release rate are obtained in the tensor form:

$$\frac{\partial \rho'}{\partial t} + \frac{\partial}{\partial x_i}\left(\bar{\rho} u'_i + \rho' \bar{u}_i\right) = 0 \tag{9}$$

$$\frac{\partial (\bar{\rho} u'_i)}{\partial t} + \frac{\partial}{\partial x_j}\left(\bar{\rho}\bar{u}_j u'_i\right) + \frac{\partial \bar{u}_i}{\partial x_j}\left(\bar{\rho} u'_j + \rho' \bar{u}_j\right) = -\frac{\partial p'}{\partial x_i} + \mu\left(\frac{\partial^2 u'_i}{\partial x_j \partial x_j} + \frac{1}{3}\frac{\partial^2 u'_j}{\partial x_i \partial x_j}\right) \tag{10}$$

$$\frac{\partial s'}{\partial t} + \bar{u}_i \frac{\partial s'}{\partial x_i} + u'_i \frac{\partial \bar{s}}{\partial x_i} = \frac{R\dot{q}'}{\bar{p}} - \frac{R\bar{\dot{q}}p'}{\bar{p}^2} + \frac{R}{\bar{p}^2}\left(\bar{p}\left(\bar{\tau}_{ij}\frac{\partial u'_i}{\partial x_j} + \tau'_{ij}\frac{\partial \bar{u}_i}{\partial x_j}\right) - p'\left(\bar{\tau}_{ij}\frac{\partial \bar{u}_i}{\partial x_j}\right)\right) \tag{11}$$

which describe the spatial-temporal evolution of the fluctuating quantities ρ', u'_i and s'. The Eq. (9) - Eq. (11) are the linearized Navier-Stokes equations (LNSE). In the Eq. (11), entropy fluctuations are chosen as the primitive variable to be solved for the linearized energy equations. Similarly, the linearized energy equation can also be formulated in terms of the pressure fluctuations, see e.g., [7].

For the state equation Eq. (7), it can be linearized for small perturbations of pressure, density and temperature. The Taylor series are developed around the mean state and only terms of the first order are kept, the linearized state equation is obtained as [10]:

$$\frac{p'}{\bar{p}} = \frac{\rho'}{\bar{\rho}} + \frac{T'}{\bar{T}} \tag{12}$$

The technique for linearization of using the Taylor series can also be applied to the entropy expression of Eq. (8). The partial derivatives of pressure with respect to density and entropy read respectively as:

$$\frac{\partial p}{\partial \rho}\Big|_{(\bar{\rho},\bar{s})} = \gamma\frac{\bar{p}}{\bar{\rho}} \tag{13}$$

$$\frac{\partial p}{\partial s}\Big|_{(\bar{\rho},\bar{s})} = \frac{\bar{p}}{C_v} \tag{14}$$

Through the linearization of the entropy expression, a relation between pressure, entropy and density fluctuations can be established:

$$\frac{p'}{\bar{p}} = \gamma\frac{\rho'}{\bar{\rho}} + \frac{s'}{C_v} \tag{15}$$

2.3 Linearized Navier-Stokes equations in frequency domain

By writing any fluctuating quantity $g'(x,t)$ as $g_1 = \hat{g}(x)e^{-j\omega t}$, one obtains the linearized Navier-Stokes equations associated with the heat release fluctuations in the frequency domain with the vector notation as below:

(16) $$\bar{\boldsymbol{u}} \cdot \nabla\hat{\rho} + \hat{\boldsymbol{u}} \cdot \nabla\bar{\rho} + \bar{\rho}\nabla \cdot \hat{\boldsymbol{u}} + \hat{\rho}\nabla \cdot \bar{\boldsymbol{u}} = j\omega\hat{\rho}$$

(17) $$\bar{\boldsymbol{u}} \cdot \nabla\hat{\boldsymbol{u}} + \hat{\boldsymbol{u}} \cdot \nabla\bar{\boldsymbol{u}} + \frac{\bar{\boldsymbol{u}} \cdot \nabla\bar{\boldsymbol{u}}}{\bar{\rho}}\hat{\rho} + \frac{1}{\bar{\rho}}\nabla\hat{p} - \frac{\mu}{\bar{\rho}}\left(\nabla^2\hat{\boldsymbol{u}} + \frac{1}{3}\nabla(\nabla \cdot \hat{\boldsymbol{u}})\right) = j\omega\hat{\boldsymbol{u}}$$

(18) $$\bar{\boldsymbol{u}} \cdot \nabla\hat{s} + \hat{\boldsymbol{u}} \cdot \nabla\bar{s} + \frac{R\bar{q}}{\bar{p}^2}\hat{p} - \frac{R}{\bar{p}}\hat{q} - \mu\left[\frac{2}{p}\nabla\bar{\boldsymbol{u}} \cdot \nabla\hat{\boldsymbol{u}} - \frac{(\nabla\bar{\boldsymbol{u}})^2}{\bar{p}^2}\hat{p} + \frac{1}{\bar{p}}\nabla\bar{\boldsymbol{u}} \cdot \nabla^T\hat{\boldsymbol{u}} + \right.$$
$$\left. \frac{1}{\bar{p}}\nabla^T\bar{\boldsymbol{u}} \cdot \nabla\hat{\boldsymbol{u}} - \frac{1}{\bar{p}^2}\nabla^T\bar{\boldsymbol{u}} \cdot \nabla\bar{\boldsymbol{u}}\hat{p} - \frac{2}{3}\left(\frac{2}{\bar{p}}(\nabla \cdot \bar{u})(\nabla \cdot \hat{u}) - \frac{(\nabla \cdot \bar{u})^2}{\bar{p}^2}\hat{p}\right)\right] = j\omega\hat{s}$$

The linearized state equation and the linearized entropy expression in the frequency domain are presented as below as well:

(19) $$\frac{\hat{p}}{\bar{p}} = \frac{\hat{\rho}}{\bar{\rho}} + \frac{\hat{T}}{\bar{T}}$$ (20) $$\frac{\hat{p}}{\bar{p}} = \gamma\frac{\hat{\rho}}{\bar{\rho}} + \frac{\hat{s}}{C_v}$$

2.4 Eigenmatrix of linearized Navier-Stokes equations

Using Eq. (19) and Eq. (20) to eliminate $\hat{p}$ in Eq. (16), Eq. (17) and Eq. (18)), one obtains the LNSE with the unknowns $\hat{\rho}$, $\hat{\boldsymbol{u}}$, $\hat{s}$. Continuity equation, momentum equation, and energy equation are presenting below respectively:

(21) $$(\bar{\boldsymbol{u}} \cdot \nabla + \nabla \cdot \bar{\boldsymbol{u}})\hat{\rho} + (\nabla\bar{\rho} + \bar{\rho}\nabla) \cdot \hat{\boldsymbol{u}} = j\omega\hat{\rho}$$

(22)
$$\left(\frac{\nabla\bar{c}^2}{\bar{\rho}} + \frac{\bar{\boldsymbol{u}} \cdot \nabla\bar{\boldsymbol{u}}}{\bar{\rho}} + \frac{\bar{c}^2}{\bar{\rho}}\nabla\right)\hat{\rho} + \left(\bar{\boldsymbol{u}} \cdot \nabla + (\nabla\bar{\boldsymbol{u}}\cdot) - \frac{\mu}{\bar{\rho}}\nabla^2 - \frac{\mu}{3\bar{\rho}}\nabla(\nabla\cdot)\right)\hat{\boldsymbol{u}} + (\gamma-1)\bar{T}\left(\frac{\nabla\bar{p}}{\bar{p}} + \nabla\right)\hat{s} = j\omega\hat{\boldsymbol{u}}$$

(23) $$\left(\frac{R\gamma\bar{q}}{\bar{p}\bar{\rho}} + \mu\left[(\nabla\bar{u})^2 + \nabla^T\bar{u} \cdot \nabla\bar{u} - \frac{2}{3}(\nabla \cdot \bar{u})^2\right]\right)\hat{\rho} +$$
$$\left((\nabla\bar{s}\cdot) - \frac{\mu R}{\bar{p}}\left[2\nabla\bar{u} \cdot \nabla + \nabla\bar{u} \cdot \nabla^T + \nabla^T\bar{u} \cdot \nabla - \frac{4}{3}(\nabla \cdot \bar{u})(\nabla\cdot)\right]\right)\hat{u}$$
$$+ \left(\bar{\boldsymbol{u}} \cdot \nabla + (r-1)\frac{\bar{q}}{\bar{p}} + \mu\left[(\nabla\bar{u})^2 + \nabla^T\bar{u} \cdot \nabla\bar{u} - \frac{2}{3}(\nabla \cdot \bar{u})^2\right]\right)\hat{s} - \frac{R}{\bar{p}}\hat{q} = j\omega\hat{s}$$

Assuming that the unsteady heat release amplitude $\hat{q}$ is modeled as a linear operator $\hat{\rho}$, $\hat{\boldsymbol{u}}$ and $\hat{s}$, formally written as $\hat{q} = q_{\hat{\rho}}\hat{\rho} + q_{\hat{\boldsymbol{u}}}\hat{\boldsymbol{u}} + q_{\hat{s}}\hat{s}$ to define the following eigenvalue problem:

(24) $$A\nu = j\omega\nu$$

with

$$A = \begin{bmatrix} \nabla \cdot \bar{\boldsymbol{u}} + \bar{\boldsymbol{u}} \cdot \nabla & \nabla \bar{p} \cdot + \bar{p} \nabla \cdot & 0 \\ \frac{\nabla \bar{c}^2}{\bar{\rho}} + \frac{\bar{\boldsymbol{u}} \cdot \nabla \bar{\boldsymbol{u}}}{\bar{\rho}} + \frac{\bar{c}^2}{\bar{\rho}} \nabla & \nabla \bar{\boldsymbol{u}} \cdot + \bar{\boldsymbol{u}} \cdot \nabla - \frac{\mu}{\bar{\rho}} \nabla^2 - \frac{\mu}{3\bar{\rho}} \nabla(\nabla \cdot) & (\gamma - 1)\bar{T} \left(\frac{\nabla \bar{p}}{\bar{p}} + \nabla \right) \\ c31 & c32 & c33 \end{bmatrix} \tag{25}$$

$$\begin{aligned} c31 &= \frac{R\gamma \bar{q}}{\bar{\rho}\bar{p}} + \mu \left[(\nabla \bar{u})^2 + \nabla^T \bar{u} \cdot \nabla \bar{u} - \tfrac{2}{3}(\nabla \cdot \bar{u})^2 \right] - \frac{R}{\bar{p}} q_{\hat{\rho}} \\ c32 &= \nabla \bar{s} \cdot - \frac{\mu R}{\bar{p}} \left[2\nabla \bar{u} \cdot \nabla + \nabla \bar{u} \cdot \nabla^T + \nabla^T \bar{u} \cdot \nabla - \tfrac{4}{3}(\nabla \cdot \bar{u})(\nabla \cdot) \right] - \frac{R}{\bar{p}} q_{\hat{\boldsymbol{u}}} \cdot \\ c33 &= \bar{\boldsymbol{u}} \cdot \nabla + (\gamma - 1)\frac{\bar{q}}{\bar{p}} + \mu \left[(\nabla \bar{u})^2 + \nabla^T \bar{u} \cdot \nabla \bar{u} - \tfrac{2}{3}(\nabla \cdot \bar{u})^2 \right] - \frac{R}{\bar{p}} q_{\hat{s}} \end{aligned}$$

The matrix Eq. (25) is the coefficient of the eigenmatrix for the proposed numerical methodology, (ω, ν) is the eigenpair, and $\nu = (\hat{\rho}, \hat{u}, \hat{s})^T$ is the eigenvector.

3. Numerical results compared with no-flow cases

In this section, numerical comparison with and without the mean flow is presented to show the influence of the flow to the thermoacoustic instabilities.

The configuration of the numerical case is one-dimensional and consists of a duct of length $L = 1$ m and with a constant cross section where the fresh gas is separated from the hot gas by flame of the thickness $\delta = 0.05$ m as Fig. 2 shows. In this case, the acoustic velocity and entropy fluctuation is zero at the inlet (i.e., $\hat{u} = 0$, $\hat{s} = 0$) and the acoustic pressure is zero as well at the outlet (i.e., $\hat{p} = 0$) [11].

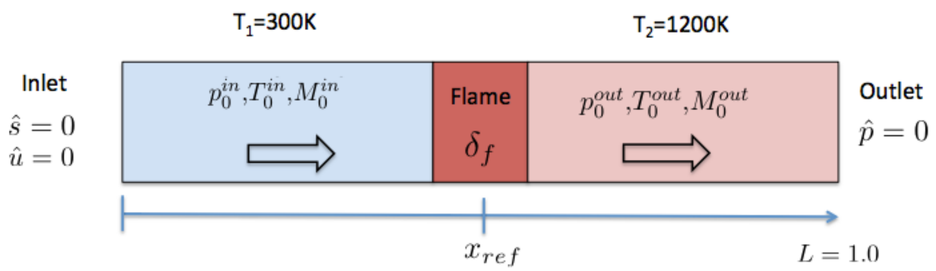

Figure 1: Numerical model for the Rijke tube case with the mean flow

When the Eq. (25) is considered without a unsteady flame, which corresponds to the case of a passive flame with zero heat release fluctuation but non-zero mean heat release. The eigenvector of passive flame is presented in Fig. 3. The influence of the mean flow to the thermoacoustic instabilities for a passive flame is shown in Fig. 4.

3.1 Mean flow calculations

The mean flow is isentropic only in regions where combustion does not occur. Due to thermal expansion, the mean flow velocity increases continuously from u_0^{in} to u_0^{out}, when the gas mixture is heated from T_0^{in} to T_0^{out}. The baseline flow is defined in order to ensure constant mass $m_0 = \rho_0 u_0$, impulsion $J_0 = p_0 + \frac{1}{2}u_0^2$ and conservation of the total temperature, viz. $\rho_0 u_0 C_p dT_{t0} dx = q_0$, with $T_{t0} = T_0 + u_0^2/(2C_p)$. More precisely the following analytical evolution for static temperature has been selected in order to mimic the presence of an anisentropic region (the flame):

$$T_0 = \frac{(T_0^{in} + T_0^{out})}{2} + \frac{(T_0^{out} - T_0^{in})}{2} \tanh\left(3\frac{x - x_f}{2\delta_f} \right) \tag{26}$$

The mean flow is then entirely determined by the choice of three independent quantities, for example the inlet pressure p_0^{in}, temperature T_0^{in} , Mach number M_0^{in}.

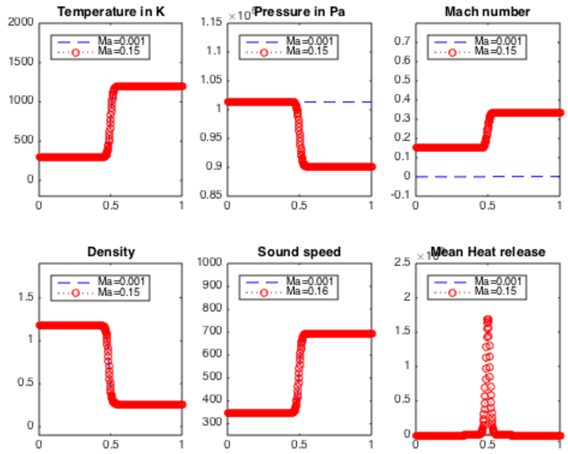

Figure 2: Mean flow field of the configuration of the flame-duct.

3.2 1d combustion with the passive flame with the mean flow effect

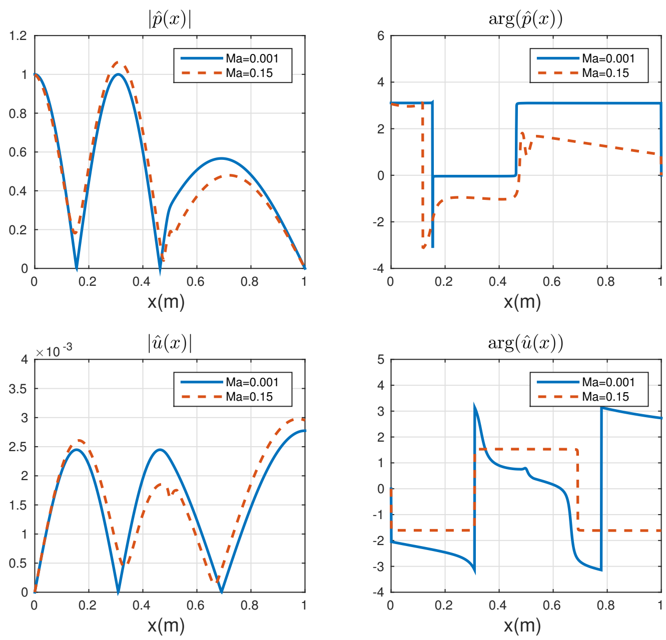

Figure 3: Structure of the third eigenmode at low and high Mach numbers as obtained numerically by the LNSE solver for $\delta_f = 0.05L$.

As shown in the Fig. 3. the mode shapes of the pressure perturbation and the velocity perturbations are ploted. The magnitude of both of them are normalized by the pressure perturbation at the inlet, thus the $|\hat{p}| = 1$ at the inlet. Three protuberance have been observed along the duct, which are determined by the wave length as well as the length of the duct. When the Mach number increases to 0.5, the mode shape are showing some disturbances at $x = 0.5$, where exactly the flame located.

The Fig. 4. shows that the eigen-frequencies of the ducted-flame system, the numerical results have been compared against the results by the semi-analytical model by Dowling [1]. In the figure,

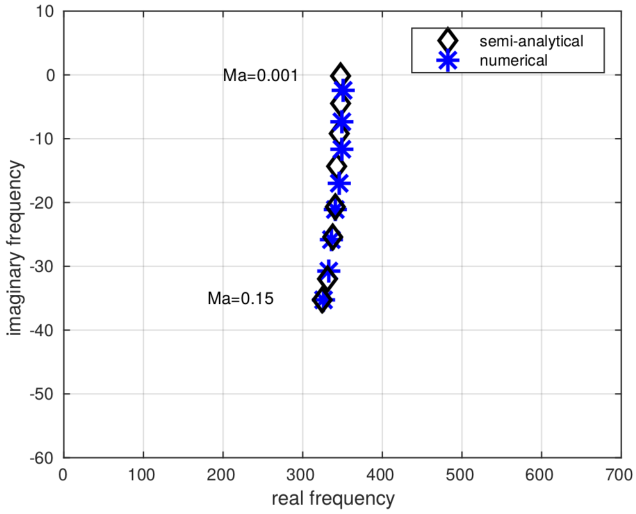

Figure 4: Mean flow effect on the thermoacoustic instabilities

the second mode of the eigen-frequencies are plotted, the imaginary parts of eigen-frequencies are more negative with the increasing Mach number, which means that the combustion process is more stable. Furthermore, it shows that mean flow effects are non-negligible, which is also one of the motivations for the current work to investigate the mean flow effect on combustion instabilities.

4. Summary and Outlook

In the paper, the numerical methodology solving linearized Navier-Stokes equation for prediction of thermoacosutic instability is presented. In the Rijke tube benchmark case, the comparison of numerical results with and without mean flow effect is provided. It is shown that the mean flow effect has an significant effect on the thermoacoustic instabilities. Further numerical work will be proceed with the proposed numerical methodology.

5. Acknowledgment

The presented work is part of the Marie Curie Initial Training Network Thermo-acoustic and aero-acoustic nonlinearities in green combustors with orifice structures (TANGO). We gratefully acknowledge the financial support from the European Commission under call FP7-PEOPLE-ITN-2012.

References

1. Ann P Dowling. The calculation of thermoacoustic oscillations. *Journal of sound and vibration*, 180(4):557–581, 1995. `https://doi.org/10.1006/jsvi.1995.0100`.

2. T Lieuwen. Modeling premixed combustion-acoustic wave interactions: A review. *Journal of Propulsion and Power*, 19(5):765–781, 2003.

3. Habib N Najm and Ahmed F Ghoniem. Coupling between vorticity and pressure oscillations in combustion instability. *Journal of Propulsion and Power*, 10(6):769–776, 1994.

4. Axel Kierkegaard, Susann Boij, and Gunilla Efraimsson. Simulations of the scattering of sound waves at a sudden area expansion. *Journal of Sound and Vibration*, 331(5):1068–1083, 2012.

5. F. Nicoud and K. Wieczorek. About the zero mach number assumption in the calculation of thermoacoustic instabilities. *International Journal of Spray and Combustion Dynamics*, 1(1):67–111, Mar 2009.

6. Dmytro Iurashev and Andrea Di Vita. A limit cycle for pressure oscillations in a gas turbine burner. In *The 21st international congress on sound and vibration*, 2014.

7. Jannis Gikadi. *Prediction of Acoustic Modes in Combustors using Linearized Navier-Stokes Equations in Frequency Space*. PhD thesis, Universitätsbibliothek der TU München, 2014.

8. John David Anderson et al. *Computational fluid dynamics*, volume 206. Springer, 1995.

9. Wolfgang Polifke, Christian Oliver Paschereit, and Klaus Döbbeling. Constructive and destructive interference of acoustic and entropy waves in a premixed combustor with a choked exit. *Int. J. Acoust. Vib*, 6(3):135–146, 2001.

10. Kerstin Wieczorek. *Numerical study of mach number effects on combustion instability*. PhD thesis, Universitätsbibliothek der TU München, 2010.

11. Franck Nicoud, Laurent Benoit, Claude Sensiau, and Thierry Poinsot. Acoustic modes in combustors with complex impedances and multidimensional active flames. *AIAA journal*, 45(2):426–441, 2007.